ARTICLE IN PRESS

Available online at www.sciencedirect.com

SciVerse ScienceDirect

Proceedings of the Combustion Institute xxx (2012) xxx–xxx

Proceedings of the Combustion Institute

www.elsevier.com/locate/proci

Turbulence–radiation interactions in large-eddy simulations of luminous and nonluminous nonpremixed flames

A. Gupta [a,1], D.C. Haworth [a,*], M.F. Modest [b]

[a] Department of Mechanical & Nuclear Engineering, The Pennsylvania State University, University Park, PA 16802, USA
[b] School of Engineering, University of California, Merced, CA 95343, USA

Abstract

Turbulence–radiation interactions (TRI) are explored in large-eddy simulations (LES) of luminous and nonluminous nonpremixed jet flames. The simulations feature a transported filtered density function (FDF) method for subfilter-scale fluctuations in composition and temperature, and a fully coupled photon Monte Carlo (PMC) method for radiative transfer with line-by-line (LBL) spectral resolution. The model is exercised to isolate and quantify individual contributions to TRI for conditions that range from small optically thin flames to relatively large optically thick flames, including spectral molecular gas radiation and broadband soot radiation. The results provide new physical insight into TRI and guidance for modeling. In all cases, emission TRI are responsible for a significant fraction of the radiative emission, and that fraction increases with increasing optical thickness. For simulations where 84% of the turbulence kinetic energy is resolved, contributions of subfilter-scale fluctuations to emission TRI exceed those of resolved-scale fluctuations. The largest contributions to emission TRI are the absorption coefficient–temperature correlation and the temperature self-correlation. Absorption TRI are evident only for relatively high optical thicknesses. In all cases, the contributions of subfilter-scale fluctuations to absorption TRI are negligible.

Keywords: Probability density function method; Filtered density function method; Large-eddy simulation; Turbulence–radiation interactions

1. Introduction

The importance of radiation heat transfer in turbulent flames, including spectral radiation properties and turbulence–radiation interactions (TRI), is increasingly being recognized. Computational models that neglect these processes, or treat them in an over-simplified manner, give inaccurate predictions of mean radiative heat fluxes, temperatures and pollutant emissions [1,2]. Radiation and TRI effects are most prominent in high-optical-thickness systems, including high-pressure, large-scale and/or luminous (sooting) flames.

Transported probability density function (PDF) methods are effective in accounting for effects of unresolved turbulent fluctuations on

* Corresponding author. Address: Department of Mechanical & Nuclear Engineering, 232 Research East Building, The Pennsylvania State University, University Park, PA 16802, USA. Fax: +1 814 865 3389.
E-mail address: dch12@psu.edu (D.C. Haworth).
[1] Current address: Rolls-Royce Corporation, Indianapolis, IN 46241, USA.

1540-7489/$ - see front matter © 2012 The Combustion Institute. Published by Elsevier Inc. All rights reserved.
http://dx.doi.org/10.1016/j.proci.2012.05.052

Please cite this article in press as: A. Gupta et al., *Proc. Combust. Inst.* (2012), http://dx.doi.org/10.1016/j.proci.2012.05.052

chemical reaction and radiation [3]. PDF methods have been used in Reynolds-averaged models to quantify TRI in nonluminous and luminous flames [4–8]. PDF methods also are being adapted to deal with subfilter-scale fluctuations in large-eddy simulation (LES) [3,9], where they often are referred to as FDF (filtered density function) methods. Few LES TRI studies have been reported to date. In [10], TRI were studied in LES of turbulent channel flow with and without reaction; only the contributions of resolved-scale fluctuations were considered. In [11], a highly sooting (40 ppm peak soot volume fraction) nonpremixed turbulent jet flame was simulated with gray radiation properties and a LES/FDF method for emission TRI; gas radiation and subfilter-scale absorption TRI were neglected. And in [12–14], contributions of unresolved scales to TRI were assessed for canonical nonreacting flows using filtered direct numerical simulations and LES without subfilter-scale models.

Here a LES/FDF model is exercised to isolate and quantify TRI in nonpremixed jet flames. A fully coupled photon Monte Carlo (PMC) method with line-by-line (LBL) spectral resolution is used for radiative transfer. Development and validation of the LES/FDF/PMC/LBL model are described in [15]. Emission and absorption TRI are examined for flames that range from small optically thin laboratory flames to large optically thick flames, and from cases that are dominated by spectral molecular-gas radiation to cases that include gas radiation and broadband soot radiation. In LES, it is important to clearly separate contributions of resolved-scale fluctuations from those of subfilter-scale fluctuations; here that is done for the first time for TRI in turbulent flames. Contributions to emission TRI and absorption TRI from resolved scales and subfilter scales are isolated, and individual contributions to emission TRI are quantified.

2. Target flame configurations

The base configuration is Sandia Flame D [16], for which extensive measurements are available. Flame D is a laboratory-scale, nonluminous piloted methane-air flame that exhibits modest radiation effects. The global radiant fraction is approximately 5%, and an optically thin radiation model is sufficient for many purposes [8]. Earlier Reynolds-averaged TRI modeling studies for Flame D include [17] (a conserved scalar/presumed PDF method) and [8] (a transported composition PDF method). Quantitative comparisons between the present model and experiment for Flame D can be found in [15]. A subset of those comparisons is provided in the Supplemental data (Fig. S1).

Table 1
Four target flame configurations. Here D_{jet} and $U_{jet,b}$ are the fuel-jet diameter and bulk velocity, respectively.

Flame	D_{jet} (mm)	$U_{jet,b}$ (m/s)	Optical thickness
D	7.2	49.6	0.049
D+soot	7.2	49.6	0.050
4D	28.8	12.4	0.248
4D+soot	28.8	12.4	0.345

Following a practice that was adopted in earlier Reynolds-averaged modeling studies [8], three other Flame-D-based configurations are simulated to access regimes where radiation and TRI are more prominent. This is done by increasing the size of the system, and/or by introducing soot. Larger flames are constructed by scaling up the dimensions of Flame D by a factor of four, while reducing the fuel and pilot velocities to maintain the same fuel-jet-based Reynolds number of 22,000. This allows a simple geometric scaling of the computational mesh to be used for all flames. The inflow turbulence quantities for the scaled-up flames are specified such that the turbulence intensity and the ratio of the turbulence integral length scale to the nozzle diameter are the same as for Flame D. Soot is introduced using a correlation (Section 3.1) that is tuned to give a maximum soot volume fraction of 4 ppm. This is high for methane-air flames, but is representative of soot levels in luminous flames [6,7]. The purpose is to provide a reasonable level of soot so that the associated radiation effects can be studied.

This gives a series of four flames that range from small, optically thin nonluminous flames to large, relatively optically thick luminous flames (Table 1). There the optical thickness is defined as the emission-weighted Planck-mean absorption coefficient times $10D_{jet}$. The radiation properties include cases that are dominated by spectral molecular gas radiation and cases with a mixture of molecular gas and broadband soot radiation. These flames cover a range of radiation environments that are relevant in practical systems.

3. Physical models and numerical methods

Aspects of the LES/FDF/PMC/LBL model that are most important for this study are described. Further details are available in [15].

3.1. Turbulent reacting flow: LES/FDF

An unstructured finite-volume method built using components from the OpenFOAM toolkit [18] is used to solve the filtered compressible continuity, momentum and energy equations using second-order spatial and temporal discretizations.

Please cite this article in press as: A. Gupta et al., *Proc. Combust. Inst.* (2012), http://dx.doi.org/10.1016/j.proci.2012.05.052

A Smagorinsky turbulent-viscosity-based subfilter-scale turbulence model is used.

The working fluid is a multicomponent reacting ideal-gas mixture. A 16-species skeletal methane-air mechanism [19] or a global one-step mechanism is used for gas-phase chemistry; the latter has been used for parametric studies. Soot is introduced via a correlation that gives the local soot volume fraction as a function of local equivalence ratio [11,20]. While this soot model has limited quantitative predictive capability, it is sufficient for the purpose of studying TRI in LES.

A transported composition PDF (FDF) method is used to account for subfilter-scale fluctuations in composition and temperature. The joint FDF of species mass fractions and mixture specific enthalpy is considered, and the modeled FDF transport equation is solved using a consistent hybrid Lagrangian particle/finite-volume method. Standard models are used for subfilter-scale turbulent transport (gradient transport) and for molecular mixing (coalescence-dispersion, with a subfilter mixing time scale). An equivalent-enthalpy approach is used for coupling the Lagrangian and Eulerian sides of the calculation through the filtered density [3,21].

3.2. Radiation and TRI: PMC/LBL

The radiation source term in the unaveraged, unfiltered energy equation is the difference between the local rate of emission and the local rate of absorption, and can be written in terms of the divergence of the radiation heat flux $\vec{q}_{rad}$. Taking the mean leads to,

$$\langle \nabla \cdot \vec{q}_{rad} \rangle = \int_0^\infty \left(4\pi \langle \kappa_\eta I_{b\eta} \rangle - \int_{4\pi} \langle \kappa_\eta I_\eta \rangle d\Omega \right) d\eta, \tag{1}$$

where,

$$\langle \kappa_\eta I_{b\eta} \rangle = \langle \kappa_\eta \rangle \langle I_{b\eta} \rangle + \langle \kappa'_\eta I'_{b\eta} \rangle,$$
$$\langle \kappa_\eta I_\eta \rangle = \langle \kappa_\eta \rangle \langle I_\eta \rangle + \langle \kappa'_\eta I'_\eta \rangle. \tag{2}$$

Here mean values are indicated by angled brackets and fluctuations by primes, η denotes wavenumber, κ_η is the spectral absorption coefficient (a known function of wavenumber, local pressure, temperature and composition), $I_{b\eta}$ is the Planck function (a known function of wavenumber and local temperature), Ω is solid angle, and I_η is the spectral radiative intensity that is obtained by solving the radiative transfer equation (RTE) [22].

The last terms on the right-hand side of Eq. (2) represent contributions of turbulent fluctuations to mean emission and mean absorption; these are manifestations of TRI. Emission TRI arise from correlations between the fluctuating absorption coefficient and the fluctuating Planck function (fourth power of temperature), which are both local quantities. Absorption TRI arise from correlations between the fluctuating absorption coefficient (determined by local quantities) and the fluctuating intensity (determined by values from the entire domain). Absorption TRI are particularly difficult to model, because of their non-local nature.

A stochastic spectral PMC method is used to solve the RTE. Notional photon bundles are emitted locally on every computational time step with wavenumbers, directions and energies that are sampled from distributions that correspond (in the limit of an infinite number of samples) to the correct local spectral rate of emission. Each photon bundle deposits energy along its trajectory based on the local absorption coefficient, until its energy is depleted to zero or it exits the computational domain. The FDF particles and the PMC particles are coupled such that effects of subfilter-scale fluctuations are captured for both emission and absorption [15]. No approximations are made regarding the directional or spatial dependence of intensity, and essentially line-by-line spectral resolution is maintained [8,23]. Here CO_2 and H_2O are considered as participating species, using spectral radiation properties from standard databases. The spectral absorption coefficient for soot is evaluated using the small-particle limit (Rayleigh theory) [22] with the complex index of refraction from [24]; scattering is neglected. Applications of these models in a Reynolds-averaged/PDF framework can be found in [6–8].

In LES, turbulent fluctuations in composition and temperature and their contributions to TRI are partially resolved. It is desirable to separate the contributions of resolved-scale fluctuations (which are captured implicitly) from those of subfilter-scale fluctuations (which must be modeled). Contributions of resolved-scale and subfilter-scale fluctuations to TRI are referred to as "ReS TRI" and "SFS TRI," respectively. These are isolated by comparing results obtained using different methods to compute emission and absorption.

Table 2
Cases to isolate TRI contributions in LES. Case names ending in "F" and "C" refer to frozen-field analysis and coupled simulations, respectively.

Case name	Emi. calc.	Abs. calc.	Emission		Absorption	
			ReS TRI	SFS TRI	ReS TRI	SFS TRI
TRI0	Mean	Mean	–	–	–	–
TRI1F	Cell	Mean	Y	–	–	–
TRI2F	Cell	Cell	Y	–	Y	–
TRI3F	Part.	Cell	Y	Y	Y	–
TRI4F	Part.	Part.	Y	Y	Y	Y
TRI2C	Cell	Cell	Y	–	Y	–
TRI3C	Part.	Cell	Y	Y	Y	–
TRI4C	Part.	Part.	Y	Y	Y	Y

Please cite this article in press as: A. Gupta et al., *Proc. Combust. Inst.* (2012), http://dx.doi.org/10.1016/j.proci.2012.05.052

The local emission and/or absorption can be calculated in one of three ways (Table 2): using time-averaged mean values of composition and temperature, thereby neglecting both ReS TRI and SFS TRI; using finite-volume cell-level (filtered) values, thereby capturing ReS TRI while neglecting SFS TRI; or using FDF particle-level values, thereby capturing both ReS TRI and SFS TRI.

Results from different radiation treatments are compared using frozen-field analysis or fully coupled simulations. In the former, a baseline LES with full TRI (emission and absorption based on FDF particle values) is run until a statistically stationary state is reached, and instantaneous cell-level and particle-level values are saved. Snapshots of emission and absorption then are calculated using either mean values, cell values or particle values. In a coupled simulation, the LES is run to a stationary state with a specified radiation treatment.

Individual contributions to TRI are isolated by comparing results from the cases listed in Table 2: ReS emission TRI by comparing cases where emission is calculated using cell (TRI1) versus mean (TRI0) values; ReS absorption TRI by comparing cases where absorption is calculated using cell (TRI2) versus mean (TRI1) values; total ReS TRI by comparing cases where emission and absorption are calculated using cell (TRI2) versus mean (TRI0) values; SFS emission TRI by comparing cases where emission is calculated using particle (TRI3) versus cell (TRI2) values; and SFS absorption TRI by comparing cases where absorption is calculated using particle (TRI4) versus cell (TRI3) values.

3.3. Model setup for target flames

Numerical parameters have been chosen based on results from earlier LES/FDF modeling studies and parametric studies in [15]. A nonuniform mesh of approximately 1.2M hexahedral cells is used. The computational domain extends from the plane of the fuel-nozzle exit to $70D_{jet}$ in the streamwise direction, and to $18D_{jet}$ in the radial direction. From the subfilter-scale turbulence model, it is estimated that 84% of the turbulence kinetic energy is resolved. Nominally 15 FDF particles are used per finite-volume cell, and approximately 4M PMC bundles are launched and traced per time step. Simulations were run using up to 128 cores of a Linux cluster with Intel Xeon E5472 quad-core 3.0 GHz processors and Mellanox DDR Infiniband (20 Gb/s) interconnect. A fully coupled LES/FDF/PMC/LBL with single-step global chemistry requires 5850 CPU hours per flow-through time (based on the fuel-jet velocity). The FDF method accounts for approximately 12% of the CPU time, and the PMC method accounts for approximately 68% of the CPU time. With the 16-species mechanism, the CPU time per flow-through time increases to 10,800 h, and the FDF and PMC methods account for approximately 53% and 35% of the CPU time, respectively.

At the inflow boundary, Flame-D-measured mean and rms velocity profiles are imposed, and a digital-filter turbulence synthesis technique [25] is used to give realistic spatial and temporal coherence. The LES/FDF/PMC/LBL simulations are initialized from a LES flow field with cell-level chemistry, and are further run for approximately three flow-through times to establish a statistically stationary state. Then time averages are accumulated over one-to-two flow-through times. Azimuthal averaging is used to reduce the statistical error in estimating mean quantities.

4. Results and discussion

Global radiation characteristics, contributions of resolved- versus subfilter-scale fluctuations to emission and absorption TRI, and a detailed breakdown of individual contributions to emission TRI are provided.

4.1. Global radiation characteristics

The global radiant fraction and the fraction of emission that is reabsorbed in the computational domain are tabulated in Table 3. Coupled simulations were run only for a subset of cases. For TRI4C (full TRI) versus TRI0 (no TRI), the radiant fraction increases from 2.8% to 4.1% for Flame D and from 22.0% to 47.8% for 4D+soot. The computed values for Flame D are lower than the experimental value of 5.1% because of the truncated

Table 3
Global radiation results.

	D	D+soot	4D	4D+soot
Radiant fraction				
TRI0	0.028	–	0.202	0.220
TRI1F	0.031	–	0.233	0.327
TRI2F	0.032	0.150	0.247	0.308
TRI3F	0.041	0.238	0.331	0.487
TRI4F	0.041	0.238	0.323	0.480
TRI2C	–	–	0.254	0.315
TRI3C	–	–	–	0.472
TRI4C	0.041	–	0.316	0.478
Fraction reabsorbed				
TRI0	0.372	–	0.618	0.483
TRI1F	0.357	–	0.612	0.422
TRI2F	0.346	0.165	0.589	0.458
TRI3F	0.332	0.120	0.566	0.383
TRI4F	0.328	0.121	0.577	0.391
TRI2C	–	–	0.583	0.458
TRI3C	–	–	–	0.397
TRI4C	0.330	–	0.583	0.391

Please cite this article in press as: A. Gupta et al., *Proc. Combust. Inst.* (2012), http://dx.doi.org/10.1016/j.proci.2012.05.052

computational domain. Radiant fractions are significantly higher for the sooting flames compared to the corresponding nonsooting flame. A large fraction of the emitted radiation is reabsorbed, in all cases. The fraction reabsorbed is smaller for the sooting flames compared to the corresponding nonsooting flame; there is more emission for the sooting flames, but there is also less absorption because the radiation properties are closer to being gray. TRI are responsible for a significant fraction of the total emission for all flames, and the fraction attributable to TRI increases with increasing optical thickness. Examples of instantaneous resolved temperature fields for Flames 4D and 4D+soot are provided in the Supplemental data (Fig. S2).

4.2. Resolved-scale and subfilter-scale TRI

Contributions of subfilter-scale fluctuations to emission TRI (TRI3 versus TRI2) exceed those of resolved-scale fluctuations (TRI2 versus TRI0) for all four flames. Differences between TRI2F and TRI1F for Flames 4D and 4D+soot suggest that absorption TRI play a role in the higher-optical-thickness flames. However, in all cases, absorption TRI are dominated by resolved-scaled fluctuations; the contributions of subfilter-scale fluctuations are very small (TRI4F versus TRI3F, or TRI4C versus TRI3C).

Examples of local TRI effects are shown in Fig. 1 (mean quantities) and Fig. 2 (instantaneous cell-level snapshots). These are for Flame 4D+soot, where TRI effects are most pronounced. There are large differences between TRI2 and TRI0 (resolved-scale TRI) and between TRI3 and TRI2 (subfilter-scale emission TRI), while results from TRI4 and TRI3 are indistinguishable (subfilter-scale absorption TRI). The differences between TRI4F and TRI2F in the frozen-field volumetric emission plotted in Fig. 2 are due to subfilter-scale emission TRI.

4.3. Breakdown of contributions to emission TRI

Local contributions of resolved-scale fluctuations to radiative emission can be quantified by taking the ratio of the local time-averaged mean emission that is computed based on the resolved temperature and composition fields to the local emission based on the mean temperature and composition fields. This ratio (denoted $ReSEmTRI_{Tot}$) can be decomposed to isolate three individual contributions of resolved-scale fluctuations: the absorption coefficient-Planck function correlation $ReSEmTRI_{\kappa T}$, the absorption coefficient self-correlation $ReSEmTRI_{\kappa}$ and the temperature self-correlation $ReSEmTRI_{T}$. Thus $ReSEmTRI_{Tot} = ReSEmTRI_{\kappa T} \cdot ReSEmTRI_{\kappa} \cdot ReSEmTRI_{T}$, where the individual terms are defined by:

$$\frac{\langle \kappa_P(\widetilde{T},\widetilde{\underline{Y}})\widetilde{T}^4\rangle}{\kappa_P(\langle\widetilde{T}\rangle,\langle\widetilde{\underline{Y}}\rangle)\langle\widetilde{T}\rangle^4} = \frac{\langle \kappa_P(\widetilde{T},\widetilde{\underline{Y}})\widetilde{T}^4\rangle}{\langle \kappa_P(\widetilde{T},\widetilde{\underline{Y}})\rangle\langle\widetilde{T}^4\rangle} \cdot \frac{\langle \kappa_P(\widetilde{T},\widetilde{\underline{Y}})\rangle}{\kappa_P(\langle\widetilde{T}\rangle,\langle\widetilde{\underline{Y}}\rangle)} \cdot \frac{\langle\widetilde{T}^4\rangle}{\langle\widetilde{T}\rangle^4}. \tag{3}$$

Here κ_P is the Planck-mean absorption coefficient, and a tilde indicates a local density-weighted filtered (cell) value. Departures of $ReSEmTRI_{Tot}$, $ReSEmTRI_{\kappa T}$, $ReSEmTRI_{\kappa}$ and/or $ReSEmTRI_{T}$ from unity are manifestations of resolved-scale emission TRI.

The analogous expression for the contributions of subfilter-scale fluctuations is: $SFSEmTRI_{Tot} = SFSEmTRI_{\kappa T} \cdot SFSEmTRI_{\kappa} \cdot SFSEmTRI_{T}$, where the individual terms are defined by,

$$\frac{\langle \widetilde{\kappa_P T^4}\rangle}{\langle \kappa_P(\widetilde{T},\widetilde{\underline{Y}})\widetilde{T}^4\rangle} = \frac{\langle \widetilde{\kappa_P T^4}\rangle\langle \kappa_P(\widetilde{T},\widetilde{\underline{Y}})\rangle\langle\widetilde{T}^4\rangle}{\langle\widetilde{\kappa_P}\rangle\langle\widetilde{T^4}\rangle\langle \kappa_P(\widetilde{T},\widetilde{\underline{Y}})\widetilde{T}^4\rangle} \cdot \frac{\langle\widetilde{\kappa_P}\rangle}{\langle \kappa_P(\widetilde{T},\widetilde{\underline{Y}})\rangle} \cdot \frac{\langle\widetilde{T^4}\rangle}{\langle\widetilde{T}^4\rangle}. \tag{4}$$

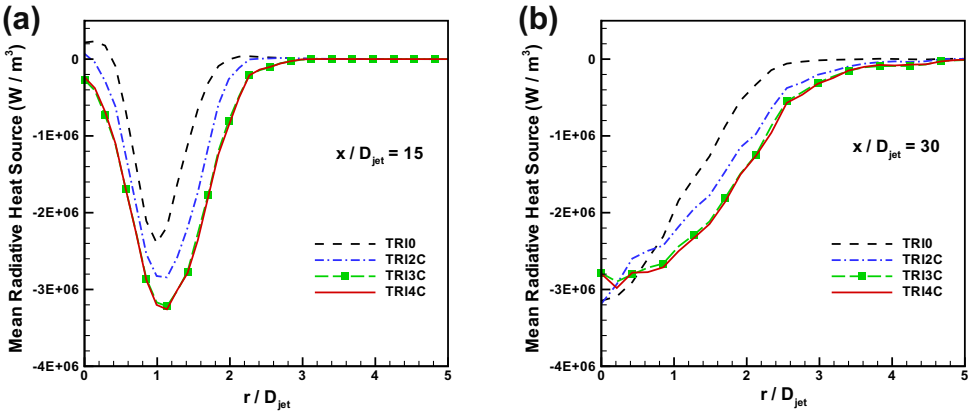

Fig. 1. Radial profiles of mean radiative heat source at two axial locations for coupled Flame 4D+soot simulations with different TRI treatments. (a) $x/D_{jet} = 15$. (b) $x/D_{jet} = 30$.

Please cite this article in press as: A. Gupta et al., *Proc. Combust. Inst.* (2012), http://dx.doi.org/10.1016/j.proci.2012.05.052

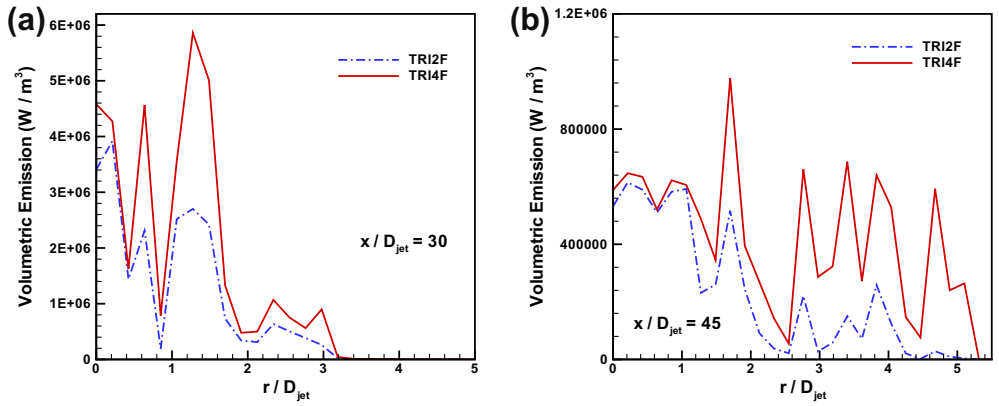

Fig. 2. Radial profiles of instantaneous resolved volumetric emission at two axial locations for a LES/FDF snapshot of Flame 4D+soot with different TRI treatments. (a) $x/D_{jet} = 30$. (b) $x/D_{jet} = 45$.

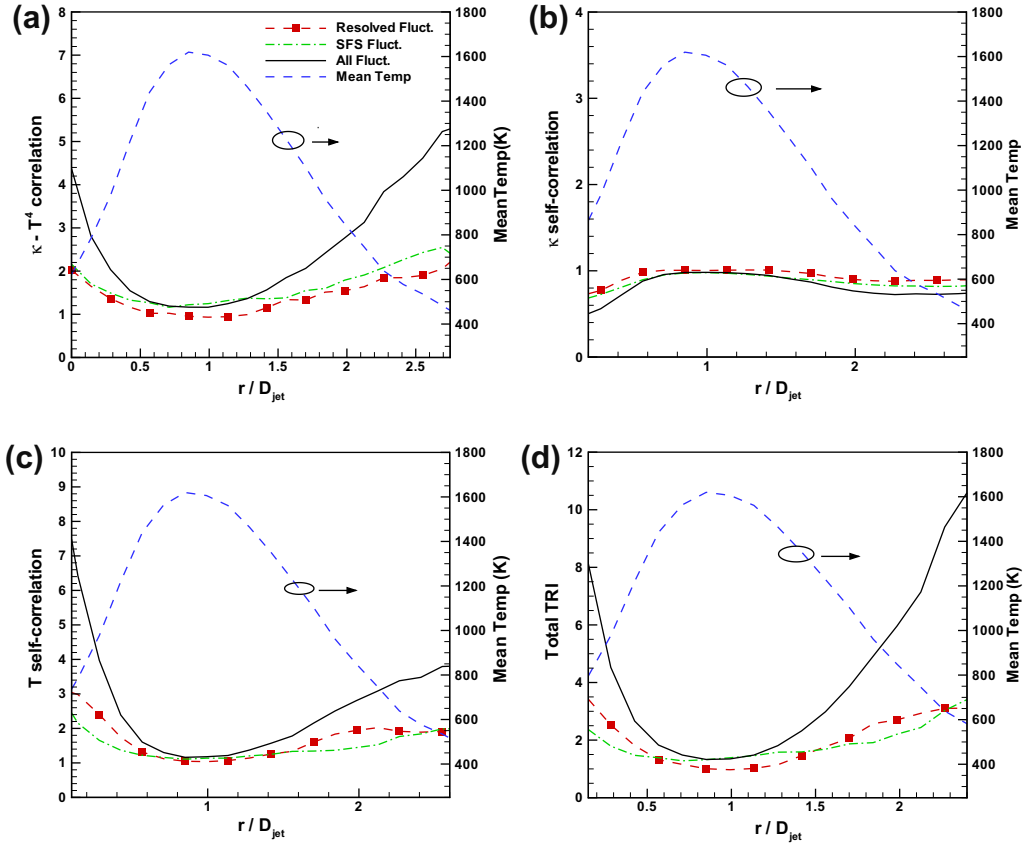

Fig. 3. Radial profiles of mean temperature and resolved-scale (Eq. (3)) and subfilter-scale (Eq. (4)) emission TRI terms for Flame 4D+soot at $x/D_{jet} = 30$. (a) $\kappa - T$ correlations, $ReSEmTRI_{\kappa T}$ and $SFSEmTRI_{\kappa T}$. (b) κ self-correlations, $ReSEmTRI_{\kappa}$ and $SFSEmTRI_{\kappa}$. (c) T self-correlations, $ReSEmTRI_{T}$ and $SFSEmTRI_{T}$. (d) Totals, $ReSEmTRI_{Tot}$ and $SFSEmTRI_{Tot}$.

Subfilter-scale fluctuations are accounted for using particle values, and the denominator of each term includes the effects of resolved-scale fluctuations. Departures of each of the individual terms in Eq. (4) from unity are manifestations of subfilter-scale emission TRI.

Please cite this article in press as: A. Gupta et al., *Proc. Combust. Inst.* (2012), http://dx.doi.org/10.1016/j.proci.2012.05.052

Radial profiles of mean temperature (for reference) and of the individual terms in Eqs. (3) and (4) are plotted at one axial location for Flame 4D+soot in Fig. 3. In each subfigure, the contributions of resolved-scale fluctuations, subfilter-scale fluctuations and all fluctuations (product of ReS and SFS terms) are plotted. The value of each term exceeds unity at most locations, which means that the net effect of that term is an increase in the local emission. An exception is the absorption-coefficient self-correlation (Fig. 3b), which is less than one at some locations (thus tending to decrease the local emission), and is always close to one. Temperature and participating-species concentration fluctuations are positively correlated (Fig. S3), and have opposing influences on the absorption coefficient. Hence the net contribution of the absorption coefficient self-correlation is small. Emission TRI are dominated by the absorption coefficient-temperature correlation and by the temperature self-correlation. In each subfigure, the magnitudes of the ReS and SFS terms are comparable at a given radial location. Since the denominator of the SFS term includes the corresponding ReS contribution (Eq. (4)), this confirms that subfilter-scale fluctuations dominate the emission TRI. Although 84% of the turbulence kinetic energy is resolved, the contributions of subfilter-scale temperature and species fluctuations to the rms temperature, rms species and temperature-species correlations are comparable to those of the resolved-scale fluctuations (Fig. S3). Similar results are found at other axial locations ([15], Figs. S4–S7).

5. Conclusions

A LES/FDF/PMC/LBL model has been exercised to isolate and quantify various contributions to TRI for a series of flames that spans a wide range of radiation environments. Flame 4D+soot has been emphasized, but the essential results and conclusions are the same for the other flames ([15], Figs. S8–S12).

Emission TRI are responsible for a significant fraction of the emission, even in small nonluminous flames. The fraction of emission attributable to TRI increases with increasing optical thickness. For LES where 84% of the turbulence kinetic energy is resolved (typical of current practice), contributions of subfilter-scale fluctuations to emission TRI exceed those of resolved fluctuations. Therefore, in cases where emission TRI cannot be neglected, it is important to include a model for subfilter-scale emission TRI. The most important terms are the absorption coefficient-temperature correlation and the temperature self-correlation.

Absorption TRI are evident only for high optical thicknesses. In all cases, absorption TRI are dominated by the resolved fluctuations; the contribution of subfilter-scale fluctuations is negligible. This is a welcome finding, because absorption TRI are particularly difficult to model. The FDF/PMC approach is the only method reported to date that is capable of capturing subfilter-scale absorption TRI. The results suggest that more conventional deterministic RTE solvers should be sufficient for most purposes in LES.

Acknowledgements

This research has been supported by NASA under Cooperative Agreement No. NNX07AB40A.

Appendix A. Supplementary data

Supplementary data associated with this article can be found, in the online version, at http://dx.doi.org/10.1016/j.proci.2012.05.052.

References

[1] M.F. Modest, *Int. J. Multiscale Comput. Eng.* 3 (2005) 85–106.
[2] P.J. Coelho, *Prog. Energy Combust. Sci.* 33 (2007) 311–383.
[3] D.C. Haworth, *Prog. Energy Combust. Sci.* 36 (2010) 168–259.
[4] S. Mazumder, M.F. Modest, *Int. J. Heat Mass Trans.* 42 (1999) 971–991.
[5] G. Li, M.F. Modest, *J. Quant. Spectrosc. Radiat. Trans.* 73 (2002) 461–472.
[6] R.S. Mehta, M.F. Modest, D.C. Haworth, *Combust. Theory Model.* 14 (2010) 105–124.
[7] R.S. Mehta, D.C. Haworth, M.F. Modest, *Combust. Flame* 157 (2010) 982–994.
[8] G. Pal, A. Gupta, M.F. Modest, D.C. Haworth, Paper No. AJTEC2011-44585, ASME/JSME 8th Thermal Engineering Joint Conference, 2011.
[9] T.G. Drozda, M.R.H. Sheikhi, C.K. Madnia, P. Givi, *Flow Turb. Combust.* 78 (2007) 35–67.
[10] A. Gupta, M.F. Modest, D.C. Haworth, *J. Heat Trans.* 131 (2009), 061704–1–8.
[11] A.J. Chandy, D.J. Glaze, S.H. Frankel, *J. Heat Trans.* 131 (2009), 051201–1–9.
[12] M. Roger, C.B. Da Silva, P.J. Coelho, *Int. J. Heat Mass Trans.* 52 (2009) 2243–2254.
[13] M. Roger, P.J. Coelho, C.B. Da Silva, *Int. J. Heat Mass Trans.* 53 (2010) 2897–2907.
[14] M. Roger, P.J. Coelho, C.B. Da Silva, *J. Quant. Spectrosc. Radiat. Trans.* 112 (2011) 1250–1256.
[15] A. Gupta, *Large-eddy simulation of turbulent flames with radiation heat transfer*, Ph.D. thesis, The Pennsylvania State University, University Park, PA, 2011.
[16] R.S. Barlow, J.H. Frank, *Proc. Combust. Inst.* 27 (1998) 1087–1095.
[17] P.J. Coelho, O.J. Teerling, D. Roekaerts, *Combust. Flame* 133 (2003) 75–91.
[18] OpenFOAM, The open source CFD toolbox, (2011). Available at http://www.openfoam.com/.

[19] S. James, M.S. Anand, M.K. Razdan, S.B. Pope, *J. Engin. Gas Turb. Power* 123 (2001) 747–756.
[20] J.P. Gore, *A theoretical and experimental study of turbulent flame radiation*, Ph.D. thesis, The Pennsylvania State University, University Park, PA, 1986.
[21] M. Muradoglu, S.B. Pope, D.A. Caughey, *J. Comput. Phys.* 172 (2001) 841–878.
[22] M.F. Modest, *Radiative Heat Transfer*, Second ed., Academic Press, New York, 2003.
[23] A. Wang, M.F. Modest, *J. Heat Trans.* 128 (2006) 1041–1049.
[24] H. Chang, T.T. Charalampopoulos, *Proc. Royal Soc. (London) A* 430 (1990) 577–591.
[25] M. Klein, A. Sadiki, J. Janicka, *J. Comput. Phys.* 186 (2003) 652–665.

Please cite this article in press as: A. Gupta et al., *Proc. Combust. Inst.* (2012), http://dx.doi.org/10.1016/j.proci.2012.05.052